ELSEVIER

NeuroImage

www.elsevier.com/locate/ynimg
NeuroImage 30 (2006) 1313 – 1324

Widespread functional connectivity and fMRI fluctuations in human visual cortex in the absence of visual stimulation

Yuval Nir,[a] Uri Hasson,[b] Ifat Levy,[b] Yehezkel Yeshurun,[c] and Rafael Malach[a,*]

[a]*Department of Neurobiology, Weizmann Institute of Science, Rehovot 76100, Israel*
[b]*Center for Neural Science, New York University, New York, NY 10003, USA*
[c]*School of Computer Science, Tel Aviv University, Tel Aviv 61390, Israel*

Received 6 May 2005; revised 9 November 2005; accepted 11 November 2005
Available online 18 January 2006

To what extent does the visual system's activity fluctuate when no sensory stimulation is present? Here, we studied this issue by examining spontaneous fluctuations in BOLD signal in the human visual system, while subjects were placed in complete darkness. Our results reveal widespread slow fluctuations during such rest periods. In contrast to stimulus-driven activity, during darkness, functionally distinct object areas were fluctuating in unison. These fMRI fluctuations became rapidly spatially de-correlated (39% drop in correlation level, $P < 0.008$) during visual stimulation. Functional connectivity analysis revealed that the slow spontaneous fluctuations during rest had consistent and specific neuro-anatomical distribution which argued against purely hemodynamic noise sources. Control experiments ruled out eye closure, low luminance and mental imagery as the underlying sources of the spontaneous fluctuations. These results demonstrate that, when no stimulus is present, sensory systems manifest a robust level of slow organized fluctuation patterns.
© 2005 Elsevier Inc. All rights reserved.

Keywords: Spontaneous activity; Ongoing activity; Rest activity; De-coherence; Functional connectivity

Introduction

To what extent can the human visual system be viewed as an information processing device that is active primarily in response to external stimuli? (Marr, 1982; Riesenhuber and Poggio, 2000) Recent studies have revealed spontaneous fluctuations in activity of the cat visual cortex which are elicited in the anesthetized animal in the absence of sensory stimuli (Kenet et al., 2003). These results have demonstrated that ongoing activity may play an important role in cortical function and cannot be ignored in exploration of cognitive processes (Tsodyks et al., 1999). Similar results have also been obtained in the alert ferret, revealing a strong correspondence between patterns of correlated neuronal activity during and in the absence of visual stimulation (Fiser et al., 2004). Finally, recent electro-physiological recordings in the alert monkey have demonstrated the existence of slow widespread coherent fluctuations (Leopold et al., 2003). Interestingly, such fluctuations were highly similar when the animal performed a visual task and during rest in a dimly lit environment, when the animal's sensory stimuli were quite restricted.

In the present study, we set out to characterize, using fMRI, the extent to which such slow (<1 Hz) neural fluctuations may occur in the human visual cortex in the absence of visual stimuli. A second aim of the present work was to obtain a direct comparison between the properties of these spontaneous fluctuations and the evoked activity which is elicited by conventional visual stimulation, thus characterizing the critical parameters that distinguish the rest fluctuations and the visually evoked activity.

Materials and methods

Subjects

Ten healthy subjects (6 women, ages 22–50) participated in one or more of the experiments (7 in the 'vision vs. darkness' experiment, 6 in the 'vision vs. fixation' experiment and in the 'full darkness experiment' and 5 in the 'control experiment' and in the 'free viewing' experiment). All subjects had normal or corrected to normal vision and provided written informed consent. The Tel-Aviv Sourasky Medical Center ethically approved the experimental protocol.

Stimuli and experimental designs

Stimuli were generated on a PC, projected via an LCD projector (Epson MP 7200) onto a tangent screen positioned over the subject's forehead and viewed through a tilted mirror.

* Corresponding author. Fax: +972 8 934 4140.
E-mail address: rafi.malach@weizmann.ac.il (R. Malach).
Available online on ScienceDirect (www.sciencedirect.com).

1053-8119/$ - see front matter © 2005 Elsevier Inc. All rights reserved.
doi:10.1016/j.neuroimage.2005.11.018

'*Vision vs. darkness*' *experiment*

The 'vision vs. darkness' experiment was 615 s long. Auditory instructions marked transitions between the darkness and visual conditions, lasting 120 s each.

In the darkness condition, all visual stimuli were extinguished, subjects were instructed to close their eyes, pay close attention to any visual-like percepts that might occur during darkness (e.g. visual-like dots) and to report it following the scan. Upon completion of the scan, subjects were interviewed to check whether (and when) they experienced any visual-like percepts during the darkness periods and whether these percepts were similar to meaningful object images (such as faces or houses) since such percepts are expected to elicit activity in high-order visual cortex (Ishai et al., 2000).

In the visual condition, subjects' eyes were open, and they were presented with visual stimuli. An interleaved short block design was used, where each visual epoch lasted 9 s followed by a 6 s blank screen. The stimuli included line drawings of faces, buildings and geometric patterns subtending 10° of visual field. Drawings were presented at medium contrast (black line drawings on uniform gray (36%) background), in an attempt to minimize after-image effects in the darkness epochs. The first epoch of every visual interval contained images of geometric patterns to ensure that the object-selective activations were not biased by a novelty effect. Nine images of the same category were presented in each epoch; each image was presented for 800 ms and was followed by a 200 ms blank screen. A central red fixation point was present throughout the visual interval. During these visual epochs, one or two consecutive repetitions of the same image occurred in each epoch, and the subject's task was to covertly report whether the presented stimulus was identical to the previous stimulus or not. The visual condition started with one epoch of patterns followed by alternating epochs of faces and buildings.

Overall, the duration and frequency of stimulation during the visual conditions were chosen for their effectiveness in activating high-order visual areas (Hasson et al., 2003; Levy et al., 2001).

'*Vision vs. fixation*' *experiment*

The 'vision vs. fixation' experiment was 615 s long, alternating between intervals of visual stimulation (120 s) and long fixation intervals (120 s). In the long fixation condition, subjects viewed a small central red fixation point superimposed on a blank (gray) screen. Subjects were instructed to pay close attention to any visual-like percepts that might occur during fixation (e.g. visual-like dots) and to report it following the scan. Subjects were interviewed (same as above) to make sure that no intense imagery of meaningful object images occurred during the long fixation periods. The visual condition was exactly identical to the visual condition described above in the 'vision vs. darkness' experiment.

'*Full darkness*' *experiment*

In the full darkness experiment, subjects' eyes were closed throughout the experiment (615 s long). Instructions were identical to those given for the shorter darkness intervals described above.

'*Control*' *experiment*

In the control experiment, subjects' eyes were closed throughout the experiment. Subjects were engaged in three different tasks: in one condition (navigation imagery), subjects imagined their daily route to work. In the second condition (mental calculation), subjects consecutively subtracted 7 starting at 1000. The third 'no-task' condition was identical to the darkness intervals in the other experiments. Subjects were trained prior to the scan for the above tasks. The entire experiment was 615 s long. Auditory instructions marked transitions between the different conditions, lasting 100 s each.

'*Free viewing*' *experiment*

In order to directly compare the present results with our previous findings, we have also re-analyzed data from a 'free viewing' experiment in which subjects viewed an uninterrupted segment from a popular movie. For details, see Hasson et al., 2004.

Data acquisition

Subjects were scanned in a 1.5 T Signa Horizon LX 8.25 GE scanner. In all experiments, a standard birdcage head coil was used, and the scanned volume included 17–27 nearly axial slices of 4 mm thickness and 1 mm gap to cover the entire cortical surface. Blood oxygenation level dependent (BOLD) contrast was obtained with gradient-echo echo-planar imaging (EPI) sequence (TR = 3000, TE = 55, flip angle = 90°, field of view 24 × 24 cm^2, matrix size 80 × 80, phase readout direction = antero-posterior).

A whole brain spoiled gradient (SPGR) sequence was acquired on each subject to allow accurate cortical segmentation, reconstruction and volume-based statistical analysis. The scanned volume included 80–120 nearly axial slices of 1.2 mm thickness to cover the entire brain volume (TR = 40, TE = 9, flip angle = 30°, field of view 24 × 24 cm^2, matrix size 256 × 256, phase readout direction = left–right). T1-weighted high resolution anatomical images of the same orientation and thickness as the EPI slices were also acquired to facilitate incorporating the functional data into the 3D space (TR = 400, TE = 14, flip angle = 90°, field of view 24 × 24 cm^2, matrix size 196 × 196, phase readout direction = antero-posterior).

Data analysis

General

fMRI data were analyzed with the BrainVoyager software package (Goebel, 2000) and with complementary in-house software. The first three volumes of each functional scan were discarded. The functional images were superimposed on 2D anatomical images and incorporated into the 3D data sets through trilinear interpolation. The complete data set was transformed into Talairach space (Talairach and Tournoux, 1988). Pre-processing of functional scans included 3D motion correction, linear trend removal, slice scan time correction and spatial smoothing using a Gaussian filter of 4 mm full width at half maximum value (FWHM). We filtered out very low frequencies (<0.0167 Hz) in the 'vision vs. darkness' data, in the 'vision vs. fixation' data and in the 'full darkness' data. Such filtering was not implemented in the control experiment since both the imagery and calculation conditions may have contained a tonic activation level lasting for the entire duration of the 100-s epoch.

The cortical surface was reconstructed from the 3D-SPGR scan. The procedure included segmentation of the white matter using a

grow-region function, the smooth covering of a sphere around the segmented region and the expansion of the reconstructed white matter into the gray matter. The surface was then unfolded, cut along the calcarine sulcus and flattened. Statistical analysis was conducted on the flattened cortex.

Statistical analysis and definitions of regions of interest (ROIs)

Throughout our statistical analysis, we assumed a hemodynamic lag of 3–6 s. In the 'full darkness' experiment, the lag was set to 3 s for all subjects since this is the default lag which is used in our studies when individual adjustments are not possible (Hasson et al., 2004). In experiments which contained visual stimulation, the lag was adjusted separately for each subject based on optimal visual activation compared to the short fixation periods.

In order to define object-selective ROIs, we created a new data set containing only the visual intervals of the 'vision vs. darkness/fixation' experiments. This was accomplished by concatenating the time courses acquired during the two visual intervals separately for each voxel, after our basic preprocessing procedures. We then performed statistical analysis based on the General Linear Model (Goebel, 1996). A box-car predictor with a delay of 3/6 s was constructed for each experimental condition except the short fixation blanks (patterns, faces, buildings), and the model was independently fitted to the time course of each voxel. A coefficient was calculated for each predictor using a least-squares algorithm.

The linear model was fitted separately for the first and second visual intervals. We used the 'internal-localizer' approach in which one part of the time course served for ROI definition, while the other part served to estimate level of activation (Lerner et al., 2002). Note that this approach guarantees the independence of the ROI definitions from the activation level measurements but ensures that ROI definitions and activation measurements are performed on data acquired during the same scanning session, in a similar fashion to the 'functional scout' method (Weilke et al., 2001).

ROIs were defined on the cortical surface as clusters of at least 50 mm^2 in which the P value of the test was less than 0.05, after correction for multiple comparisons (see below). Face-selective ROIs included voxels which showed significantly higher activation to faces vs. buildings (faces > buildings contrast), in the vicinity of the fusiform gyrus (pFs—also known as the fusiform face area—FFA (Kanwisher et al., 1997)) and in the inferior occipital gyrus (IOG) (Hasson et al., 2003). Building-selective ROIs included voxels which showed significantly higher activation to buildings vs. faces (buildings > faces contrast), in the vicinity of the collateral sulcus (CoS—likely corresponding to the parahippocampal place area—PPA (Epstein and Kanwisher, 1998)) and in the transverse occipital sulcus (TOS) (Hasson et al., 2003). To avoid confusion with various naming schemes, we will refer to the face- and building-related regions in ventral occipito-temporal cortex as FFA and PPA respectively.

Calculation of significance values in the activation map (Fig. 1B) was based on the individual voxel significance and on the minimum cluster size of 50 mm^2 voxels (Forman et al., 1995). A correction for multiple comparisons was performed by calculating the probability of a false positive from the frequency count of cluster sizes within the entire cortical surface, using a Monte Carlo simulation (AlphaSim by B. Douglas Ward, a software module in Cox, 1996). Finally, multi-subject maps (Fig. 1B) were generated using random effect analysis.

Vision and rest comparisons

Time courses for Figs. 1C and D were sampled from the building-selective PPA separately for each subject. The multi-subject average time course (Fig. 1C) was created by first converting, separately for each subject, the BOLD time course to percent signal change values. We used the average response during the short fixation periods as a baseline for the percent signal change conversion. These time courses were then averaged across subjects.

Time courses in the Supplementary Figs. 2 and 6 were sampled from four object-selective regions in the occipito-temporal cortex of both hemispheres: the PPA and TOS building-related regions, and the FFA and IOG face-related regions (Hasson et al., 2003).

For one subject (subject NZ), there was no significant building-selective activity in the transverse occipital sulcus during the 'vision vs. fixation' experiment, and this time course is absent in Supplementary Fig. 6.

All tests comparing visual stimulation periods and darkness periods (Fig. 2) were conducted separately on time courses sampled from these four regions bilaterally.

The power spectrum (Fig. 2 and Supplementary Fig. 3) was defined as the base-10 logarithm of the squared absolute value of the FFT components. Significant differences in the power spectrum were defined by a paired t test ($P < 0.05$) separately for each frequency range ([0.017 Hz–0.025 Hz–0.033 Hz–0.042 Hz–0.05 Hz–0.058 Hz–0.067 Hz–0.075 Hz–0.083 Hz–0.092 Hz–0.1 Hz–0.108 Hz–0.117 Hz–0.125–0.133 Hz–0.142 Hz–0.15 Hz–0.158 Hz–0.167 Hz]). The same power spectrum analysis was used to compare the spectral content of the darkness intervals of the 'vision vs. darkness' experiment to the 'full darkness' data (Supplementary Fig. 4). For this purpose, we used segments with identical length (120 s) from the 'full darkness' data.

Functional connectivity during rest

Functional connectivity results (Fig. 3A and Supplementary Fig. 5) were generated by defining two 'seed' time courses sampled from the building-related PPA of the left hemisphere and the inferior parietal cortex (IPC) of the right hemisphere. Each time course was used as a GLM predictor to compute a voxel-by-voxel fit (analogous to linear correlation). This fit was evaluated after removing the auto-regression factor (BrainVoyager software package (Goebel, 2000)) since consecutive fMRI data points of the regressor are not statistically independent due to the nature of the hemodynamic response.

For Fig. 3B, we applied a random effect group analysis in order to further examine the neuro-anatomical distribution of the rest fluctuations. In contrast to the normally applied procedure, in which every subject's data set is fitted with the same design matrix, we used a different design matrix for each data set, based on the subject's actual data ('seed' time courses from the same ROIs) so that the final map reflects regions which are consistently highly correlated to the same 'seed' location across subjects.

Correlations and spatial de-coherence index

After defining 2 face- and 2 building-selective regions in each hemisphere (Hasson et al., 2003), we calculated, using the 'internal

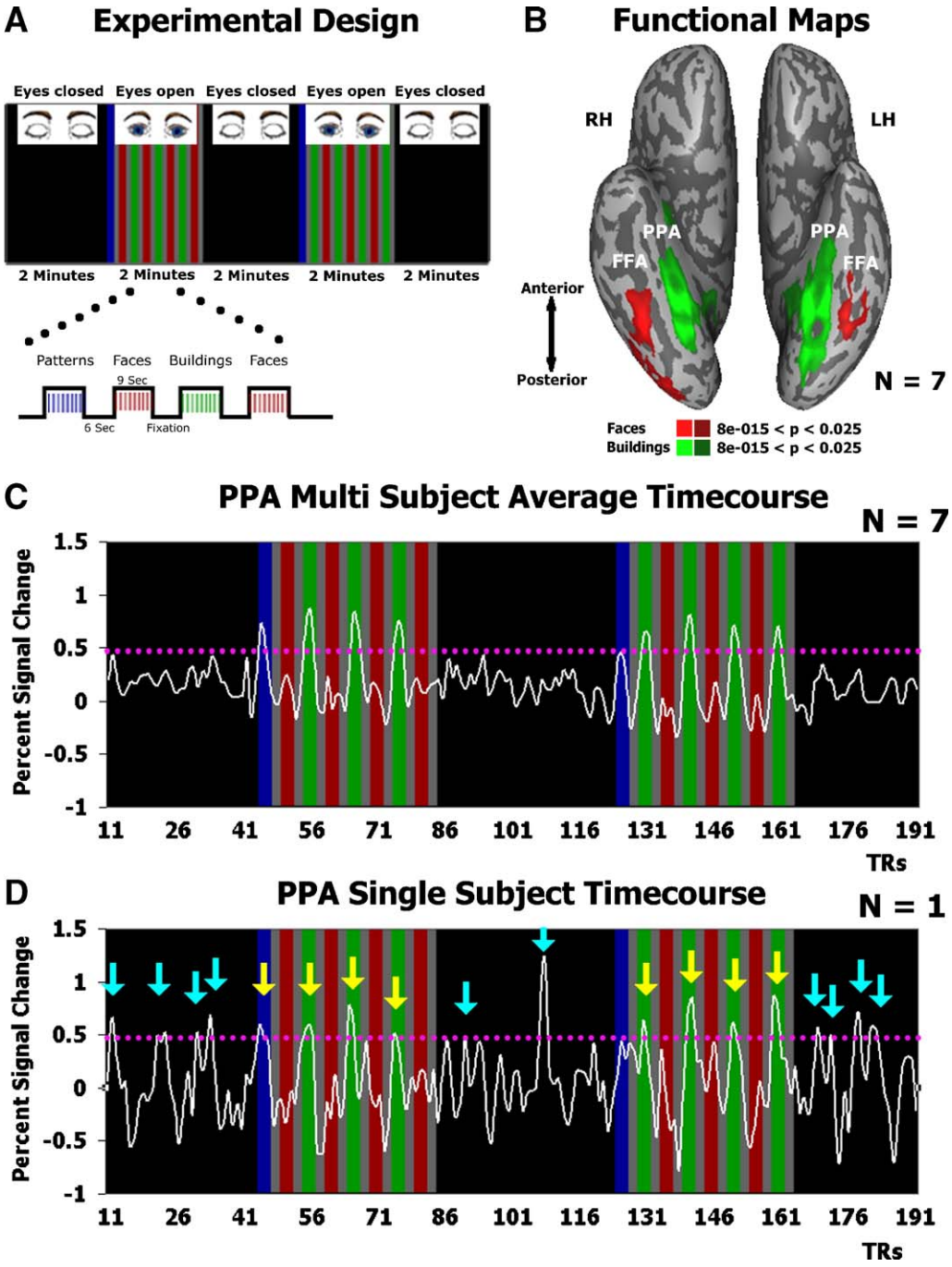

Fig. 1. 'Vision vs. darkness' experiment. (A) Experimental design. (B) Functional maps shown on an inflated cortical surface (ventral view). Red (green) areas mark face (building)-selective regions. LH, left hemisphere; RH, right hemisphere; FFA, fusiform face area; PPA, parahippocampal place area. (C) PPA average time course showing multi-subject average activity in terms of percent signal change from short fixation baseline epochs. Purple dotted line marks 75% of average building-selective response. Note that in the group data it seems that there are no strong peaks during darkness. Prior to averaging, single subject time courses were shifted by 3–6 s to account for the hemodynamic lag. (D) PPA single subject time course: purple dotted line marks 75% of average building-selective response. Yellow and cyan arrows mark peaks during vision and darkness, respectively. Note that in single subject data strong peaks are quite frequent during darkness. This time course was shifted by 3 s to account for the hemodynamic lag.

localizer' approach, the linear correlation coefficients between an average time course of a given region to average time courses of all other regions in the same hemisphere. Coefficients were then averaged into 3 groups (Figs. 4A and C): 'Face–Face' correlations denote correlations between the FFA and the IOG face-related regions. Similarly, 'Building–Building' correlations mark correlations between the PPA and the TOS building-related regions. Finally, 'Face–Building' correlations represent an average of all the 4 across-category correlations. Significance levels were obtained by applying a paired t test comparing F–F (or B–B) to F–B correlations ($P < 0.05$).

Spatial de-coherence level was defined as the difference between the within-category correlation (an average of the F–F and B–B values) to the across-category correlation (F–B value).

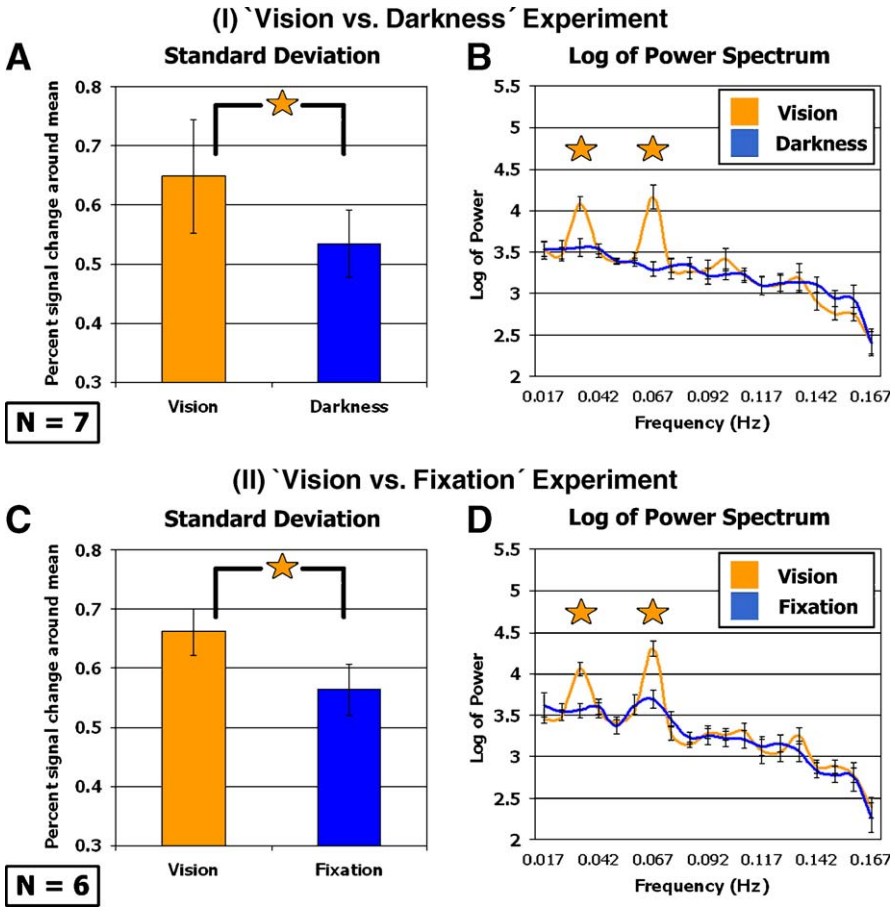

Fig. 2. 'Characteristics of object regions' time courses. (I) 'Vision vs. darkness' experiment. (A) The standard deviation of time course values was significantly higher during visual stimulation (paired t test, $P < 0.05$, $n = 7$), indicating a larger modulation depth. (B) Log of power spectrum. Significant differences were found only for the visual stimulation frequencies (paired t test, $P < 0.05$, $n = 7$). (II) 'Vision vs. fixation experiment. (C) The standard deviation of time course values was significantly higher during visual stimulation (paired t test, $P < 0.05$, $n = 6$), indicating a larger modulation depth. (D) Log of power spectrum. Significant differences were found only for the visual stimulation frequencies (paired t test, $P < 0.05$, $n = 6$). Every parameter of interest was computed for all selective object areas and then averaged across regions and subjects. Statistical significance was evaluated by comparing the 'vision' and 'darkness'/'fixation' values for a given subject. Error bars mark inter-subject standard error of the mean ($n = 7/6$).

Dynamic spatial de-coherence (Figs. 4B and D) was computed by using a moving window of ±10 time points around a center data point and calculating the spatial de-coherence value for each of the 21-point intervals. Thus, for each time point t, the value computed is:

$$\frac{\left(r\langle A,B\rangle_{t-10}^{t+10}+r\langle C,D\rangle_{t-10}^{t+10}\right)}{2}-\frac{\left(r\langle A,C\rangle_{t-10}^{t+10}+r\langle A,D\rangle_{t-10}^{t+10}+r\langle B,C\rangle_{t-10}^{t+10}+r\langle B,D\rangle_{t-10}^{t+10}\right)}{4}$$

where: A = FFA, B = IOG, C = PPA, D = TOS, and $r\langle A, B\rangle_{T1}^{T2}$ denotes the linear correlation coefficient between A and B for the interval [T1 T2].

Analysis of control experiment data

Map of different tasks during darkness (Fig. 5A) was obtained by contrasting each condition with the other two (e.g. imagery vs. calculation and 'no-task') via GLM. Contours of building-related regions were defined according to the visual interval of the 'vision vs. darkness' experiment, while borders of retinotopic areas are schematic for illustration purposes only.

For the standard deviation analysis (Fig. 5B), we sampled time courses of activation from the FFA and PPA and converted the signals to percent signal change values around the mean prior to calculation of the standard deviation.

For the spatial de-coherence analysis (Fig. 5C), we combined data from several different experiments in the following manner: (i) for the 'imagery', 'no-task' and 'mental calculation' conditions, data were collected from the control experiment ($n = 5$), and ROIs were defined as follows: face-selective regions were defined by an external localizer, using the 'vision vs. darkness' experiment. Imagery-activated regions, located slightly anterior to the standard building-selective regions (Fig. 5A), were defined by using the 'internal localizer' method (Lerner et al., 2002). (ii) For the 'block design' condition, we present data from the visual intervals of the 'vision vs. darkness' experiment ($n = 7$), as seen in Fig. 4A, while ROIs were defined using the 'internal localizer' approach. (iii) For the motion picture condition, we present data from the free viewing experiment (Hasson et al., 2004). ROIs were externally defined

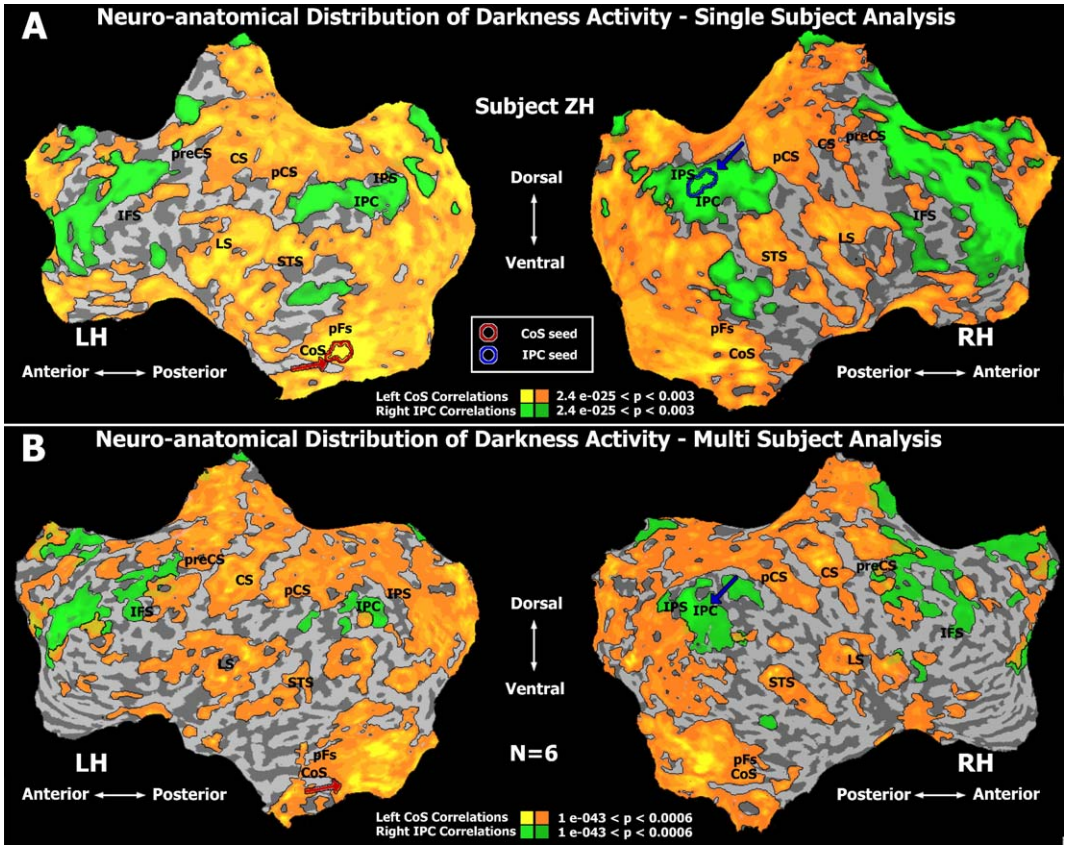

Fig. 3. Neuro-anatomical distribution of rest activity. (A) Single subject analysis. Neuro-anatomical distribution of single subject rest activity shown on flattened cortical hemispheres. Orange areas mark highly correlated regions to the left PPA (red contour) in the collateral sulcus. Green areas mark highly correlated regions to the right IPC (blue contour). CoS, collateral sulcus; pFs, posterior fusiform gyrus; STS, superior temporal sulcus; IPC, inferior parietal cortex; IPS, inferior parietal sulcus; LS, lateral sulcus; IFS, inferior frontal sulcus; preCS, pre-central sulcus; CS, central sulcus; pCS, post-central sulcus; LH, left hemisphere; RH, right hemisphere. (B) Group analysis. Neuro-anatomical distribution of rest activity as revealed by multi-subject (n = 6) random effect GLM analysis. Coloring and naming conventions are identical to panel A.

according to the visual intervals of the 'vision vs. darkness' experiments.

Results

Comparing fluctuations of activity in high-order visual cortex during vision and darkness

To what extent does the human visual system become silent when no visual input is available? We explored this issue by performing a simple experiment which consisted of two main conditions: visual stimulation and darkness (Fig. 1A). Upon completion of the experiment, one of the seven subjects reported sporadic experiences of 'visual-like' dots during darkness but could not pinpoint the exact timings of these percepts. Another subject reported some after-images in the first few seconds of the darkness condition. The rest of the subjects did not report any 'visual-like' experiences during darkness, and none of them experienced any object-like percepts during darkness.

In the visual condition, subjects' eyes were open, and they received blocks of rapid visual stimulation consisting of either pattern, face or house images. The visual epochs reproduced successfully the well-established selective organization of occipito-temporal cortex (Fig. 1B), revealing highly significant face- and building-selective regions in both hemispheres (Hasson et al., 2003). Face-selective activations were found in the FFA (Kanwisher et al., 1997) and in the IOG face-related regions (Hasson et al., 2003), while building-selective activations were found in the PPA (Epstein and Kanwisher, 1998) and in the TOS dorsally (Hasson et al., 2003). This functional selectivity was apparent not only in the multi-subject maps (Fig. 1), but also in single-subject maps obtained from each of the subjects individually (Supplementary Fig. 1A).

Fig. 1C depicts the time course of activation averaged across seven subjects derived from the PPA. Note that the averaged time course yielded a typical pattern of high activation during visual stimulation and low levels of activity during the darkness periods (Fig. 1C). However, this typical pattern changed dramatically when single subject data were inspected (Fig. 1D). Here, the darkness periods contained spontaneously emerging fluctuation peaks which were spread over large cortical expanses.

The appearance of the spontaneous fluctuations could be observed in every high level object area tested. To illustrate the ubiquity of the phenomenon, we present the entire set of time courses obtained from eight object areas (two face-related and two place-related in each hemisphere) of 7 subjects (Supplementary Fig. 2).

A quantitative comparison of object-selective activation time courses acquired during vision and during darkness revealed a significant increase in the standard deviation during visual stimulation (Fig. 2A) compared to rest, indicating that both signal

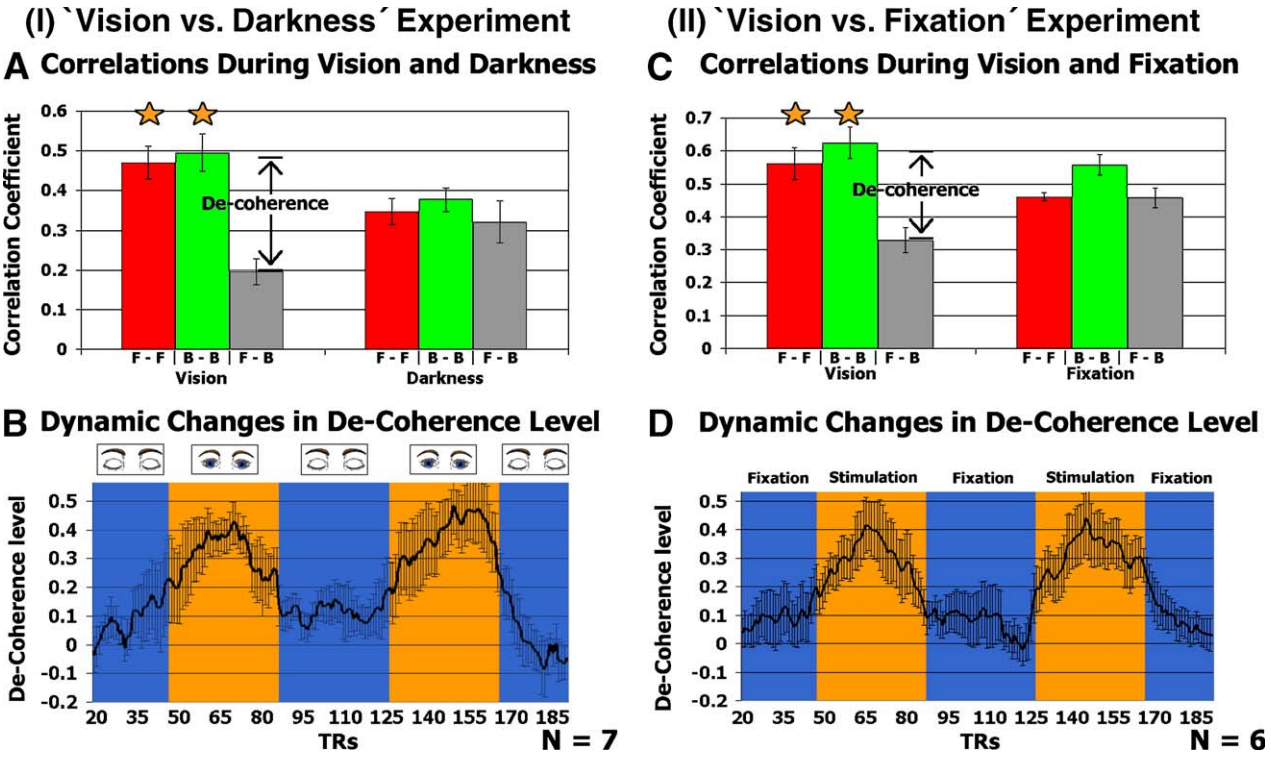

Fig. 4. Spatial de-coherence during vision, darkness and long fixation. (I) 'Vision vs. Darkness' Experiment. (A) Correlations during vision and darkness between cortical regions which are grouped by their functional properties. Note how correlation levels were uniform during darkness, while, during vision, within-category correlations (F–F, B–B) were significantly higher than across-category correlations (F–B), indicating selective processing. F, face; B, building. (B) Dynamic changes in spatial de-coherence level defined as the difference between within-category correlations to across-category correlations. Note the robust and dramatic changes corresponding to vision and darkness. (II) 'Vision vs. Fixation' Experiment. (C) Correlations during vision and long fixation between cortical regions which are grouped by their functional properties. Note how correlation levels were uniform during the long fixation, while, during vision, within-category correlations (F–F, B–B) were significantly higher than across-category correlations (F–B), indicating selective processing. F, face; B, building. (D) Dynamic changes in spatial de-coherence level defined as the difference between within-category correlations to across-category correlations. Note the robust and dramatic changes corresponding to vision and long fixation. Error bars in all panels mark inter-subject standard error of the mean (n = 6 or n = 7).

peaks and inhibitory minima were of higher amplitude during visual stimulation, thus reflecting an enhancement of the modulation depth. Analyzing the spectral content of the time courses of visual stimulation and rest did not reveal significant differences other than the expected peaks at the visual stimulation frequencies (Fig. 2B, see Supplementary Fig. 3A for individual spectra). In order to verify that the rest fluctuations were not a mere side-effect of the periodic structure of the visual stimulation, we further compared the spectral contents of the rest fluctuations during the 'vision vs. darkness' experiment to rest fluctuations recorded during a full darkness scan. The results demonstrate that the general spectral content of the rest fluctuations was maintained, regardless of prior visual stimulation (Supplementary Fig. 4).

Functional connectivity during rest

To verify that the spontaneous BOLD fluctuations during darkness indeed represented, at least partially, neuronal processes, we placed subjects in complete darkness for the entire scan and explored the neuro-anatomical distribution of their rest fluctuations by examining correlation patterns to specific cortical "seed" locations.

Fig. 3A illustrates a typical case for a "seed" located in the building-related PPA, which was chosen as an example of a high-order visual area. During rest, the PPA's signal fluctuations were highly correlated to the entire visual system. Moreover, other non-visual sensory regions, including auditory cortex, as well as regions in pre-frontal cortex, were also part of the highly correlated network, indicating that the correlated fluctuations were not limited to occipito-temporal cortex (Fig. 3).

The functional connectivity analysis in each hemisphere revealed two consistent networks which showed complete de-coupling during rest (Fig. 3, see Supplementary Fig. 5 for individual brains). The results reveal a separate network linked to inferior parietal cortex (IPC) structures, whose foci were intrinsically correlated (green patches, Fig. 3) but which showed strong de-coupling (correlation coefficient = 0.06, P = 0.39) from the rest activity of the visual system.

Furthermore, our data revealed a highly significant correlation in symmetric "mirror" locations across hemispheres (e.g. left and right PPA). These symmetric inter-hemispheric connectivity patterns were quite consistent, as can be seen in the group analysis (Fig. 3B), or by examining the individual patterns (Supplementary Fig. 5).

Overall, the segregation to two consistent networks within hemispheres and the symmetric correlations across hemispheres indicate that the fluctuations during darkness were likely due to neuronal processes (see also discussion below).

Spontaneous fluctuations during long periods of fixation

To examine whether the spontaneous fluctuations were unique to darkness periods or whether they may have been associated with

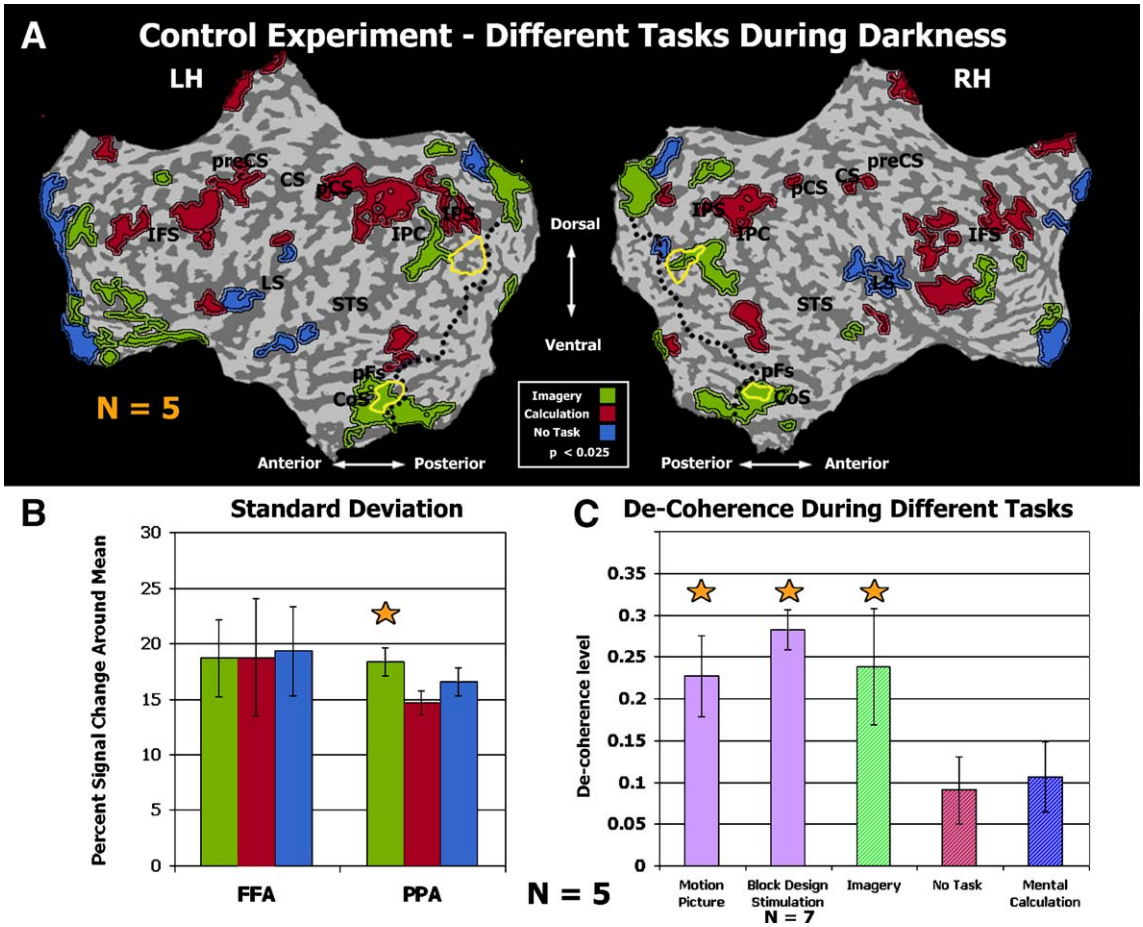

Fig. 5. Control experiment. (A) Activations during darkness averaged across 5 subjects shown on flattened cortical hemispheres. Colors indicate GLM contrast of each condition with the other two (e.g. imagery vs. calculation and no-task). Black dotted lines denote schematic borders of retinotopic regions for illustration purposes, while yellow contours mark loci of building-related regions. Note that imagery activated extensive regions, overlapping building-related regions in ventral occipito-temporal cortex and regions anterior to the building-related regions in dorsal occipito-temporal cortex. See Fig. 3 for anatomical abbreviations. (B) Standard deviation of time course values in the FFA and PPA across the different conditions. Note that enhanced standard deviation was found in the PPA during navigation imagery (paired t test, $P < 0.05$, $n = 5$), while such an effect could not be found in the FFA. (C) Spatial de-coherence levels during the different conditions of the control experiment and during different setups. Spatial de-coherence during visual stimulation and imagery was significantly higher than that found during mental calculation and passive rest (t test, $P < 0.05$). Error bars in panels B and C mark inter-subject standard error of the mean ($n = 5/7$).

any removal of complex visual stimuli, we conducted a separate experiment in which we replaced the darkness periods with the presentation of a blank screen containing a small fixation point that the subjects fixated for extended (120 s) durations. As in the darkness periods, subjects did not report any perceptions of meaningful object-like images during these prolonged fixation periods.

The results of this experiment conducted on 6 subjects are shown in the bottom panels of Fig. 2. As can be seen, the basic phenomenon of widespread spontaneous BOLD fluctuations can be evident in this experiment as well. A quantitative summary of the data obtained from similar regions of interest as in the 'visual vs. darkness' experiment confirms this impression. In a similar fashion to the 'vision vs. darkness' results, the standard deviation of the fluctuations during vision was significantly higher than during fixation (Fig. 2C). The entire set of face- and building-related time courses are provided in order to further illustrate the results (Supplementary Fig. 6). We could not find significant differences in the spectral content (other than the expected peaks at the visual stimulation frequencies) when comparing the visual condition and the long fixation condition (Fig. 2D, Supplementary Fig. 3B for individual spectra).

Post-stimulation "refractory" period

It is important to emphasize that the high-amplitude spontaneous fluctuations did not occur with equal probability throughout the rest periods. Quantitative analysis of the entire data set revealed a clear-cut "refractory" period following the termination of the visual stimuli in which no high amplitude fluctuations were evident. Thus, our results show that the average delay between the end of visual stimulation and the first high-amplitude spontaneous peak was 22.8 ± 1.2 s for darkness periods and 26.8 ± 1.6 s for fixation periods.

Spatial de-coherence

A consistent parameter that differentiated vision from darkness in the fMRI data was the level of 'spatial coherence' between functionally distinct visual areas: during darkness, such areas were

fluctuating in unison, revealing widespread coherent modulations of activity shared by the entire visual cortex. In contrast, during vision, (i) functionally similar areas were more correlated, while (ii) functionally dissimilar regions became de-correlated. We use the term 'spatial de-coherence' to indicate this difference between the within-category correlations and the across-category correlations.

Fig. 4A (arrow) illustrates the quantitative estimate of the de-coherence measure for two face- and two building-related regions (Hasson et al., 2003). As can be seen, the de-coherence values differed significantly ($P < 3E-05$) between the vision and darkness periods. Fig. 4B illustrates the waxing and waning of the spatial de-coherence level and its relation to the alternation between vision and darkness. Similar results were obtained for the 'vision vs. fixation' experiment (Figs. 4C and D).

Possible sources of rest fluctuations

Fig. 5A demonstrates that the experimental tasks employed in our control experiment (mental calculation, navigation-related mental imagery and passive rest) differentially activated specific cortical regions.

Examining activity elicited in the FFA did not show a significant difference between mental calculation and rest in terms of the standard deviation (Fig. 5B), suggesting that alpha waves may not be a major source of the rest fluctuations (see also Discussion section below).

Next, we checked whether the rest fluctuations were related to mental imagery by examining the activity elicited by the navigation imagery condition in the PPA. Although a larger standard deviation was observed (Fig. 5B), a closer inspection of the activity in regions activated by the imagery task ((i) the PPA ventrally and (ii) a region anterior to the building-related TOS dorsally), compared to the activity in neighboring face-related regions, revealed that the enhanced BOLD activation was highly de-coherent, i.e. resembled the visual activation condition (Fig. 5C), rather than the darkness fluctuations which were more coherent in nature. Finally, we have also found comparable high levels of spatial de-coherence during continuous free viewing of a popular movie (Hasson et al., 2004) (Fig. 5C, 'Motion Picture'). This suggests that spatial de-coherence is not a derivative of our specific experimental design or choice of stimuli.

Discussion

The neuronal basis of the rest fluctuations

Our results demonstrate that, during complete darkness with eyes closed, in the complete absence of visual stimuli, occipito-temporal object cortex shows consistent widespread spontaneous fluctuations.

Since fMRI does not measure the neuronal activity directly, BOLD fluctuations can arise from a diversity of sources that are not directly related to the underlying neural activity. Such sources include periodic cardiac and respiratory noise, slow autonomous hemodynamic regulation and magnetic field drift. Hence, great caution must be exercised when interpreting spontaneous fluctuations which are not phase-locked to the experimental manipulation.

We predicted that, if the spontaneous fluctuations are largely due to neuronal processes, then the functional connectivity analysis should reveal consistent patterns that cannot be explained by common hemodynamic regulation. To that end, we investigated connectivity patterns related to two 'seed' time courses—the PPA building-related region in high-order visual cortex and the IPC. The latter seed was chosen because a network linked to this region has been previously reported to be functionally connected during the resting state (Greicius et al., 2003).

Several arguments support a neuronal origin to the BOLD fluctuations during rest. First, the highly structured correlation maps (Fig. 3) and the cortical sites showing complete decoupling (green patches, Fig. 3) argue against global hemodynamic modulations which affect the entire cortex. The anatomical locations of these heterogeneous patterns of correlations were quite consistent across subjects (Supplementary Fig. 5). The strong segregation into two distinct networks is intriguing, and we are currently exploring the nature of this segregation and the functionality of these networks (Golland et al., 2005).

Second, there was an extremely high inter-hemispheric correlation between "mirror" cortical sites (Fig. 3 and Supplementary Fig. 5) which, due to the hemispheric segregation of the blood supply, is quite unlikely to reflect purely hemodynamic modulations. Furthermore, both the inter-hemispheric symmetry and the intra-hemispheric segregation to two networks could not be explained by a common posterior cerebral artery (PCA) circulation since this artery supplies the medial part of the brain (Barr and Kierman, 1993), while highly correlated regions, such as the lateral–occipital complex, were also found on the lateral surface.

One study (van de Ven et al., 2004) characterized functional connectivity in the resting state using spatial ICA. Their results differ from our data in the sense that unilateral clusters were found in the left and right IPC, suggesting that these regions may not be highly correlated across hemispheres during rest, but this discrepancy may be related to their decomposition of each data set to a relatively large number of independent components.

Thus, we conclude that the rest fluctuations were mainly caused by neuronal activity rather than spontaneous hemodynamic fluctuations—with the inter-hemispheric correlations likely mediated by the dense network of callosal connections.

Previous studies have used a similar approach to assess functional connectivity and have shown correlated signal changes during prolonged rest in various cortical regions (Biswal et al., 1995; Cordes et al., 2000; Lowe et al., 1998; Xiong et al., 1999). Our results extend previous works demonstrating that spontaneous physiological processes are likely to be the dominant factor underlying fluctuations in the BOLD signal at rest (Hoshi et al., 1998; Kruger and Glover, 2001; Peltier and Noll, 2002).

Although it is difficult to relate fast processes at the cellular level to the slower global dynamics which we measure with fMRI, the present results are compatible with many electro-physiological studies which all point to high levels of activity in the visual cortex in the absence of visual stimulation, both in the anesthetized cat (Kenet et al., 2003), in the alert ferret (Fiser et al., 2004) and in the alert monkey (Leopold et al., 2003).

Finally, further studies will be necessary in order to accurately derive neuronal behavior from the amplitude of fMRI fluctuations during rest. As we have argued elsewhere (Avidan et al., 2002), the fact that the fMRI signal is a composite of the activity of a large number of neurons in each voxel may mask substantial differences in the patterns of neuronal activations. Thus, one may get a similar amplitude of fMRI signal both as a result of a slight, but widely

distributed, increase in the activity of many individual neurons or, alternatively, as a result of an intense firing of a small group of neurons within the imaged voxel. Thus, although superficially similar, the activity during visual stimulation and during rest may be derived from completely different activation profiles at the single neuron level.

Spontaneous fluctuations during fixation

The use of complete darkness with eyes closed was helpful in assuring that no stray light could have allowed rudimentary visual processing. However, our results demonstrate that the rest fluctuations were not unique to eye closure or extremely low level of illumination since long periods of fixation were also associated with spontaneous fluctuations which were of similar profile to the darkness periods (compare Fig. 2: upper and lower panels). These results also argue against imagery as a source of the spontaneous fluctuations since visual imagery is reduced during fixation (Ishai and Sagi, 1995). We can conclude that the spontaneous fluctuations emerge in high-order visual areas whenever complex visual stimuli are absent.

Relation to previous findings

Given that comparing visual activation to fixation or a blank field is a widely used paradigm (including in our own research), it may appear surprising that such spontaneous fluctuations during rest were not observed previously. Most likely, this is due to the long "refractory" time, which we found to occur after the cessation of visual stimulation, during which no high activity fluctuations were elicited. In our specific stimulation paradigm, this period was typically longer than 20 s, which is above the typical rest period employed by most fMRI studies of the visual system. Thus, the shorter fixation or rest periods commonly used may have not permitted sufficient time for the slow spontaneous fluctuations to emerge.

A related phenomenon may be the reduced activation level which was found during the rest period interspersed between the visual stimulation epochs (indicated by gray bands in Figs. 1C–D) compared to the extended no-stimulus conditions. This lower baseline could be the result of the well known signal undershoot which typically occurs after intense stimulation (Boynton et al., 1996).

Another possibility is that long periods of rest, in contrast to short periods with intervening visual stimuli, have allowed subjects to enter a state of "reduced vigilance", similar in nature to sleep stages 1/2. However, the fact that the spontaneous fluctuations were found also during prolonged fixation and in every rest interval for each one of our subjects strongly argues against this possibility.

The variance of the spontaneous fluctuations

Our results show that the variance of the responses during visual stimulation was higher compared to the rest fluctuations (Figs. 2A, C, and Supplementary Figs. 2 and 6). These results demonstrate that both excitatory and inhibitory peaks were of higher amplitude during stimulation. Thus, enhanced variance in the fMRI signal over time, which corresponds to a larger modulation depth, appears to be an important factor distinguishing sensory-evoked activity from ongoing activity.

Spatial de-coherence

Our results show that, in the absence of visual stimulation, the entire visual system manifests slow widespread synchronized fluctuations. In contrast, visual stimulation leads to spatial de-coherence, i.e. the breakdown of overall synchrony into patterns of both strong and weak correlations between different functional regions, reflecting their functional specialization. Spatial de-coherence can be best described as a state in which BOLD fluctuations are strongly correlated between functionally similar cortical regions and weakly correlated between functionally dissimilar cortical regions.

The de-coherence during periods of object-selective visual stimuli is expected and has been demonstrated in a large number of mapping studies (Grill-Spector and Malach, 2004). However, the new finding is that this de-coherence is strongly diminished when visual stimuli are extinguished—due to the replacement of regionally selective activations by the widespread regionally synchronized peaks of slow fMRI fluctuations. This spatial coherence was evident both in complete darkness (Fig. 4A) and during long periods of fixation (Fig. 4C), indicating that spontaneous fluctuations were indeed due to the lack of structured visual stimuli, and not the result of reduced overall luminance.

We have also found comparable high levels of spatial de-coherence during continuous free viewing of a popular movie (Hasson et al., 2004) (Fig. 5C). Note that, in contrast to conventional block-designed paradigms, in which spatial de-coherence is largely expected, the free viewing paradigm is not specifically designed to activate the face- and building-related regions in alternation and thus demonstrates the generality of this phenomenon. We suggest that this state of activity, in which functionally similar areas are intrinsically correlated, while dissimilar areas are uncorrelated, is an important characteristic of sensory processing.

Our results extend recent studies which have demonstrated that functional connectivity patterns in sensory systems are significantly different during task execution or stimulation and during rest. For example, visual stimulation has been shown to increase correlations between functionally related regions and decrease correlations between regions which are not functionally related (Bartels and Zeki, 2005; Hampson et al., 2004). Similary, Broca's area and Wernicke's area increase their functional connectivity during a listening task compared to rest (Hampson et al., 2002). In the motor system, it has been suggested that the recruitment of neurons to perform a specific task may moderately reduce the degree of connectivity within and between regions (Morgan and Price, 2004). However, since various artifacts can bias correlational analyses of fMRI data (Lowe et al., 1998), our results are unique in comparing the resting state fluctuations with a state of sensory stimulation and task execution within the same scanning session.

Functional role of rest fluctuations

One may wonder what could be the mechanism underlying the rest fluctuations. One possibility could be visual imagery, which has been reported to activate the visual system during darkness (Ishai et al., 2000; O'Craven and Kanwisher, 2000). Another is the mechanism underlying enhanced EEG alpha band power associated with relaxed eye closure (Berger, 1929).

Our control experiments indicate that visual imagery could not be related to these fluctuations since, where present, it produces higher spatial de-coherence than the passive darkness state (Fig. 5C). In that respect, visual imagery appears to be more akin to visual activation than to rest fluctuations. Furthermore, in cases where imagery activation was likely to be reduced—e.g. in the face-related FFA during intense navigation imagery—we found no reduction in the rest fluctuations (Fig. 5B). Finally, the fact that we found similar spontaneous fluctuations during long fixations also argues against visual imagery as the source of these fluctuations since imagery is significantly reduced when the eyes are open (Ishai and Sagi, 1995).

Other potential correlates of the rest fluctuations may be processes related to alpha waves since spatial de-coherence is reminiscent of EEG de-synchronization and alpha "block" associated with enhanced alertness. However, the lack of significant effects associated with mental calculation, which often causes alpha disruption (Gevins and Schaffer, 1980), argues against this interpretation.

Nevertheless, it is possible that alpha "block" failed to elicit distinguishable differences in the standard deviation of the BOLD signal of high-order visual areas. A full clarification of this issue necessitates a direct comparison of EEG activity and fMRI recordings (Laufs et al., 2003), which was not undertaken in the present study. Such works demonstrated mixed results, exhibiting both positive (Moosmann et al., 2003) and negative (Laufs et al., 2003) correlation of the EEG alpha predictor with fMRI activity of the occipital lobe. It seems that further research will be needed in order to resolve the relation of surface EEG recordings during rest to the spontaneous BOLD fluctuations.

A possible role for these slow fluctuations maybe analogous to that of the slow oscillations in cortical activity found during slow-wave sleep, which may be related to memory consolidation and mechanisms of plasticity through cortico-thalamic networks (Huber et al., 2004; Steriade and Timofeev, 2003). Oscillations of a similar nature have also been observed in developing neural circuits where correlated fluctuations occur with a periodicity on the order of minutes (Feller, 1999). Another possibility is that such fluctuations represent top–down influences related to goals or expectations (Engel et al., 2001).

Thus, this study extends previous works which have demonstrated the incessant, ongoing activity in human cortex, regardless of the perceptual states. Upon stimulation, the slow widespread spontaneous fluctuations which encompass the entire visual system are replaced by regionally selective activation patterns which reflect the functional selectivity of the different visual regions. Thus, different levels of spatial de-coherence mark the transitions from the stimulated state to rest periods.

Acknowledgments

This study was funded by the AMN foundation, the Academy of Science Center of Excellence for Applied Geometry, ISF 8009 and the Benoziyo Center for Neurological Disorders. We would like to thank the fMRI unit in the Tel-Aviv Sourasky Medical Center, Dan Drai for help with dynamic spatial de-coherence analysis, Michal Harel for 3D brain reconstruction and Eli Okon for technical assistance. We thank Rainer Goebel, Moshe Bar, Amos Arieli, Leon Deouell, Sharon Gilaie-Dotan, Yulia Golland, Roy Mukamel, Galia Avidan and Amir Amedi for fruitful discussions and comments.

Appendix A. Supplementary data

Supplementary data associated with this article can be found in the online version at doi:10.1016/j.neuroimage.2005.11.018.

References

Avidan, G., Hasson, U., Hendler, T., Zohary, U., Malach, R., 2002. Analysis of the neuronal selectivity underlying low fMRI signals. Curr. Biol. 12, 964–972.

Barr, M.L., Kierman, J.A., 1993. The Human Nervous System–An Anatomical Viewpoint. J.B. Lippincott Company, Philadelphia, pp. 379–393.

Bartels, A., Zeki, S., 2005. Brain dynamics during natural viewing conditions—A new guide for mapping connectivity in vivo. NeuroImage 24, 339–349.

Berger, H., 1929. On the electroencephalogram in man. Arch. Psychiatr. Nervenkr. 87, 527–543.

Biswal, B., Yetkin, F.Z., Haughton, V.M., Hyde, J.S., 1995. Functional connectivity in the motor cortex of resting human brain using echo-planar MRI. Magn. Reson. Med. 34, 537–541.

Boynton, G.A., Engel, S.A., Glover, G., Heeger, D., 1996. Linear systems analysis of functional magnetic resonance imaging in human V1. Int. J. Neurosci., 4207–4221.

Cordes, D., Haughton, V.M., Arfanakis, K., Wendt, G.J., Turski, P.A., Moritz, C.H., Quigley, M.A., Meyerand, M.E., 2000. Mapping functionally related regions of brain with functional connectivity MR imaging. AJNR Am. J. Neuroradiol. 21, 1636–1644.

Cox, R., 1996. AFNI: software for analysis and visualization of functional magnetic resonance neuroimages. Comput. Biomed. Res. 29, 162–173.

Engel, A.K., Fries, P., Singer, W., 2001. Dynamic predictions: oscillations and synchrony in top–down processing. Nat. Rev., Neurosci. 2, 704–716.

Epstein, R., Kanwisher, N., 1998. A cortical representation of the local visual environment. Nature 392, 598–601.

Feller, M.B., 1999. Spontaneous correlated activity in developing neural circuits. Neuron 22, 653–656.

Fiser, J., Chiu, C., Weliky, M., 2004. Small modulation of ongoing cortical dynamics by sensory input during natural vision. Nature 431, 573–578.

Forman, S.D., Cohen, J.D., Fitzgerald, M., Eddy, W.F., Mintun, M.A., Noll, D.C., 1995. Improved assessment of significant activation in functional magnetic-resonance-imaging (Fmri)—Use of a cluster-size threshold. Magn. Reson. Med. 33, 636–647.

Gevins, A.S., Schaffer, R.E., 1980. A critical review of electroencephalographic (EEG) correlates of higher cortical functions. CRC Crit. Rev. Bioeng. 4, 113–164.

Goebel, R., 1996. Brain Voyager: a program for analyzing and visualizing functional and structural magnetic resonance data sets. NeuroImage 3, S604.

Goebel, R., 2000. BrainVoyager. Brain Innovation, Masstricht, The Netherlands.

Golland, Y., Bentin, S., Hasson, U., Malach, R., 2005. Bipartite Organization of the Human Caudal Brain. Paper presented at: Annual Meeting of the Organization of Human Brain Mapping (Toronto, Ontario, Canada).

Greicius, M.D., Krasnow, B., Reiss, A.L., Menon, V., 2003. Functional connectivity in the resting brain: a network analysis of the default mode hypothesis. Proc. Natl. Acad. Sci. U. S. A. 100, 253–258.

Grill-Spector, K., Malach, R., 2004. The human visual cortex. Annu. Rev. Neurosci. 27, 649–677.

Hampson, M., Peterson, B.S., Skudlarski, P., Gatenby, J.C., Gore, J.C., 2002. Detection of functional connectivity using temporal correlations in MR images. Hum. Brain Mapp. 15, 247–262.

Hampson, M., Olson, I.R., Leung, H.C., Skudlarski, P., Gore, J.C., 2004. Changes in functional connectivity of human MT/V5 with visual motion input. NeuroReport 15, 1315–1319.

Hasson, U., Harel, M., Levy, I., Malach, R., 2003. Large-scale mirror-symmetry organization of human occipito-temporal object areas. Neuron 37, 1027–1041.

Hasson, U., Nir, Y., Levy, I., Fuhrmann, G., Malach, R., 2004. Intersubject synchronization of cortical activity during natural vision. Science 303, 1634–1640.

Hoshi, Y., Kosaka, S., Xie, Y., Kohri, S., Tamura, M., 1998. Relationship between fluctuations in the cerebral hemoglobin oxygenation state and neuronal activity under resting conditions in man. Neurosci. Lett. 245, 147–150.

Huber, R., Ghilardi, M.F., Massimini, M., Tononi, G., 2004. Local sleep and learning. Nature 430, 78–81.

Ishai, A., Sagi, D., 1995. Common mechanisms of visual-imagery and perception. Science 268, 1772–1774.

Ishai, A., Ungerleider, L.G., Haxby, J.V., 2000. Distributed neural systems for the generation of visual images. Neuron 28, 979–990.

Kanwisher, N., McDermott, J., Chun, M.M., 1997. The fusiform face area: a module in human extrastriate cortex specialized for face perception. J. Neurosci. 17, 4302–4311.

Kenet, T., Bibitchkov, D., Tsodyks, M., Grinvald, A., Arieli, A., 2003. Spontaneously emerging cortical representations of visual attributes. Nature 425, 954–956.

Kruger, G., Glover, G.H., 2001. Physiological noise in oxygenation-sensitive magnetic resonance imaging. Magn. Reson. Med. 46, 631–637.

Laufs, H., Krakow, K., Sterzer, P., Eger, E., Beyerle, A., Salek-Haddadi, A., Kleinschmidt, A., 2003. Electroencephalographic signatures of attentional and cognitive default modes in spontaneous brain activity fluctuations at rest. Proc. Natl. Acad. Sci. U. S. A. 100, 11053–11058.

Leopold, D.A., Murayama, Y., Logothetis, N.K., 2003. Very slow activity fluctuations in monkey visual cortex: implications for functional brain imaging. Cereb. Cortex 13, 422–433.

Lerner, Y., Hendler, T., Malach, R., 2002. Object-completion effects in the human lateral occipital complex. Cereb. Cortex 12, 163–177.

Levy, I., Hasson, U., Avidan, G., Hendler, T., Malach, R., 2001. Center–periphery organization of human object areas. Nat. Neurosci. 4, 533–539.

Lowe, M.J., Mock, B.J., Sorenson, J.A., 1998. Functional connectivity in single and multislice echoplanar imaging using resting-state fluctuations. NeuroImage 7, 119–132.

Marr, D., 1982. Vision: A Computational Investigation Into the Human Representation and Processing of Visual Information. Freeman, New York.

Moosmann, M., Ritter, P., Krastel, I., Brink, A., Thees, S., Blankenburg, F., Taskin, B., Obrig, H., Villringer, A., 2003. Correlates of alpha rhythm in functional magnetic resonance imaging and near infrared spectroscopy. NeuroImage 20, 145–158.

Morgan, V.L., Price, R.R., 2004. The effect of sensorimotor activation on functional connectivity mapping with MRI. Magn. Reson. Imaging 22, 1069–1075.

O'Craven, K., Kanwisher, N., 2000. Mental imagery of faces and places activates corresponding stimulus-specific brain regions. J. Cogn. Neurosci. 12, 1013–1023.

Peltier, S.J., Noll, D.C., 2002. T(2)(*) dependence of low frequency functional connectivity. NeuroImage 16, 985–992.

Riesenhuber, M., Poggio, T., 2000. Models of object recognition. Nat. Neurosci. 3, 1199–1204.

Steriade, M., Timofeev, I., 2003. Neuronal plasticity in thalamocortical networks during sleep and waking oscillations. Neuron 37, 563–576.

Talairach, J., Tournoux, P., 1988. Co-planar Stereotaxic Atlas of the Human Brain. Thieme Medical Publishers, New York.

Tsodyks, M., Kenet, T., Grinvald, A., Arieli, A., 1999. Linking spontaneous activity of single cortical neurons and the underlying functional architecture. Science 286, 1943–1946.

van de Ven, V.G., Formisano, E., Prvulovic, D., Roeder, C.H., Linden, D.E., 2004. Functional connectivity as revealed by spatial independent component analysis of fMRI measurements during rest. Hum. Brain Mapp. 22, 165–178.

Weilke, F., Spiegel, S., Boecker, H., von Einsiedel, H.G., Conrad, B., Schwaiger, M., Erhard, P., 2001. Time-resolved fMRI of activation patterns in M1 and SMA during complex voluntary movement. J. Neurophysiol. 85, 1858–1863.

Xiong, J., Parsons, L.M., Gao, J.H., Fox, P.T., 1999. Interregional connectivity to primary motor cortex revealed using MRI resting state images. Hum. Brain Mapp. 8, 151–156.